9th Asia-Pacific Conference on Wind Engineering
Auckland, New Zealand
3-7 December 2017

Study on Interference Effect of Square Cylinders by Large Eddy Simulation

Y.C. Li[1], Y.L. Lo[2] and F.M. Fang[3]

[1]Wind Engineering Research Center
Tamkang University, New Taipei City, 220, Taiwan (R.O.C.)

[2] Department of Civil Engineering
Tamkang University, New Taipei City, 220, Taiwan (R.O.C.)

[3] Department of Civil Engineering
National Chung Hsing University, Taichung, 402, Taiwan (R.O.C.)

Abstract

In this study, an idealized 2D FSI simulation with LES model is attempted to simulate the 3D prism interference effect through the motion transform method instead of 3D simulation. Three typical arrangements are employed for the comparison of the aero-elastic model response trajectory. Although the absolute values from CFD results are not perfectly in good agreements with the experimental results, the movement mechanism of the aero-elastic model has consistent trend. This provides an intuitive and preliminary way for the observation of the interference mechanism.

Introduction

2D LES model had been worked successfully on vortex shedding from a bluff body flow (Bouris [2]; Noda [5]). Asyikin [1] investigated the flow characteristics and vortex induced vibration of a cylinder by means of LES model. Vikram [6] conducted a numerical investigation of two dimensional unsteady flows passing two square cylinders with in-line arrangements. These previous studies have showed that the 2D LES model can present flow-structural-iteration (FSI) mechanism fairly well.

Generally speaking, 3D FSI simulation is much more convincing but time-consuming choice for the comparison with experimental results. To overcome this disadvantage, an idealized 2D FSI simulation with LES model is attempted to simulate the 3D prism interference effect through the motion transform method in this study. Three typical arrangements simulation are employed for the comparison of the aero-elastic model response trajectory.

Problem Description

According to the Lo [3] experimental results, three identical and typical interference arrangements are simulated in this study. As Figure 1 shows, an interfering model is placed near the aero-elastic model with the distance in the along-wind (x) and across-wind (y) direction. Minus x means the interfering model is placed at the upstream of aero-elastic model. The reduced velocity is calculated as

$$U_r = \frac{\bar{U}_H}{f_0 D} \tag{1}$$

where $\bar{U}_H$ is the mean wind velocity at the model height, f_0 is fundamental frequency, D is prism width.

These three cases are (x/D, y/D) = (2, 2) at U_r = 12.5, and 15.9 and (x/D, y/D) = (-2, 0) at U_r = 15.9. In these three cases, the principal building model is observed to vibrate severely in the lateral direction due to interference effects (Lo [3]).

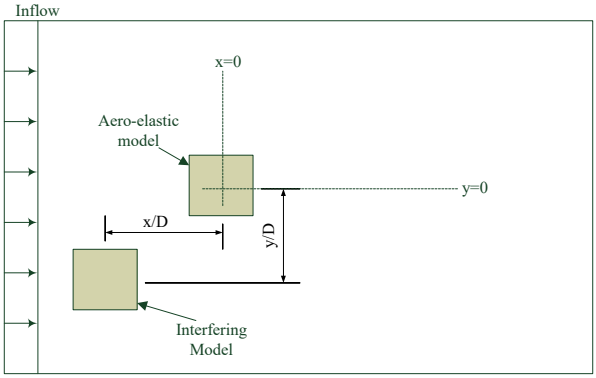

Figure 1 Diagram of setup between interfering model and aero-elastic model.

Numerical Methodology

A 2D FSI numerical simulation is conducted to enhance the understanding of the aforementioned critical cases either in the upstream or in the downstream. The CFD environment is idealized to be a 2D analysis with those identified structural characteristics and the flow condition at model height.

Structural model

A two-way coupling motion is required between the fluid and the structure. For an efficient calculation, a partitioned procedure was chosen. The fluid–structure algorithm was the same as that of the Conventional Sequential Staggered (CSS) procedure. In the present work, the response of the square cylinder was calculated using a forced mass–spring–damper equation. For the along-wind or across-wind motion, the governing equation can be written as:

$$\ddot{x}_i + 2\xi\omega_n\dot{x}_i + \omega_n^2 x_i = \frac{F_i}{m} \tag{2}$$

where i is directional index; m is mass per unit length; ξ is the damping ratio; ω_n is the circular natural frequency. The time-dependent force F was obtained by integrating the pressure over the surface of the principal model. The structural parameters identified in previous discussions were substituted for calculation. The commercial package ANSYS Fluent 15 serves as the tool for the 2D fluid-structure-interaction simulation in this study. The default solver, which provides at largest six degree-of-freedom calculations, computes external forces and moments on the specified object by integrating pressure and shear stresses over the

surface. Additional loading conditions can be added by user defined functions (UDF).

The dynamic meshing module in ANSYS Fluent 15 was adopted to simulate the surrounding grids of the principal model. In regard to dynamic meshing, the integral form of the conservation equation for a general scalar ϕ on an arbitrary control volume V, whose movable boundary can be defined as

$$\frac{d}{dt}\int_V \rho\varphi dV + \int_{\partial V}\left(\vec{u}-\vec{u}_g\right)\cdot d\vec{A} = \int_{\partial V}\Gamma\nabla\varphi\cdot d\vec{A} \quad (3)$$

where ρ is the fluid density, $\vec{u}$ is the flow velocity vector, $\vec{u}_g$ is the mesh velocity of the moving mesh, Γ is the diffusion coefficient. The integral limit ∂V represents the boundary of the control volume. By using a first-order backward difference formula, the (n+1)-th time level volume, V^{n+1}, is computed from

$$V^{n+1} = V^n + \frac{dV}{dt}\Delta t \quad (4)$$

For the second-order differencing scheme, the dot product $\vec{u}_{gj}\cdot\vec{A}_j$ on each control volume face in the volume time derivative part is calculated from

$$\vec{u}_{gj}\cdot\vec{A}_j = \frac{\delta V_j}{\Delta t} \quad (5)$$

Then the dot product $\vec{u}_{gj}\cdot\vec{A}_j$ on each control volume face is calculated by

$$(\vec{u}_{gj}\cdot\vec{A}_j)^{n+1} = \frac{3}{2}\left(\frac{\delta V_j}{\delta t}\right)^n - \frac{1}{2}\left(\frac{\delta V_j}{\delta t}\right)^{n-1} \quad (6)$$

where δV_j^n and δV_j^{n-1} are the volumes swept out by control volume faces at the current and previous time levels over a time step. The re-meshing method was used in the dynamic meshing module. Once the new cells satisfies the skewness criterion (Default: 0.7), the mesh is locally updated with the interpolated new cells from the old cells.

Adopted numerical approaches for calculation

The QUICK (Quadratic Up wind Interpolation for Convective Kinematics) scheme was used for spatial discretization of the convective terms and a bounded central difference scheme was used for the diffusive terms of the momentum equations. PISO (Pressure-Implicit with Splitting of Operators) algorithm was selected as the pressure–velocity coupling scheme for its robust convergence advantage. The time discretization was carried out by a second-order accurate fully implicit scheme. The time duration for initializing the calculation of all cases was set to 50,000 time steps and the time step size of 0.0001 sec was adopted for computation, which satisfies the Courant–Friedrichs–Lewy (CFL) and the grid Fourier criteria. With the aforementioned setting, the algebraic equations were solved by the Gauss–Siedel point-by-point iterative method in conjunction with the Algebraic Multigrid (AMG) method solver. The AMG method can greatly reduce the number of iterations required to obtain a converged solution, particularly when the model contains a large number of control volumes. The convergence criteria for the inner (time step) iterations were set as 10^{-5} for all the discretised governing equations. The dynamic Smagorinsky–Lilly model was chosen for sub-grid-scale (SGS) model (Lilly [4]).

The dimensions of the computational domain were 35D × 12D, with two square cylinders arranged at 6D downstream from the inlet where D is the cylinder's depth. The simulation domain was discretised by a non-uniform unstructured grid with a finer grid distribution near the cylinders to capture the viscous boundary layer as well as the wake and the vortex street behind the cylinders. The structured grid near the cylinders was constructed with a minimum grid space of 0.05D and extruded 10 layers normal to each cylinder surface. The y+ was less than 50 on the cylinders. Figure 2 shows the grid distribution of the 2D domain for the case (x/D, y/D) = (-2, 0). Grids are generated by using the grid generation software POINTWISE. The total grid number is about 12,000.

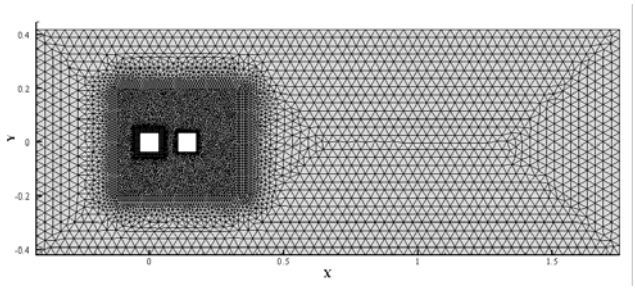

Figure 2. Grid distribution of the case (x/D, y/D) = (-2, 0).

Modification of 2D Structural Motion

In Lo's [3] experiment, a rigid base-pivoted square prism model is manufactured for the role of the principal building. The model is 0.07 m in both width (D) and depth and 0.56 m in height (H), which make the aspect ratio (D/H) 8. The fundamental frequency f is identified as 6.3 Hz in both along-wind (f_x , longitudinal) and across-wind (f_y , lateral) directions based on free vibration tests; the structural damping ratios, ζ_x and ζ_y, are estimated 0.77% in x and 0.73% in y. The generalized mass M is 0.15 kg.

Basically, 3D aero-elastic model rotates with the floor as the fulcrum. For 2D FSI simulation, the consideration turns the traverse motion equation (2) into rotational motion. The moment of inertia of the model is 0.26 kg-m^2. The structural setup is shown in Table 1. The rational deformation, velocity and are obtained from equation (1) every time step. The deformation is determined by the rational motion, which multiplies by the building height (H) to feedback the dynamic mesh of CFD.

Moment of inertia I_x, I_y	0.26 kg-m^2
Frequency f_x	6.3 Hz
Frequency f_y	6.3 Hz
Damping Ratio ζ_x	0.73 %
Damping Ratio ζ_y	0.73 %

Table 1.The aero-elastic model setup for FSI simulation.

Results

Figure 3-5 are plotted for three critical cases compared with the corresponding arrangements in experimental results. The case at (-2, 0) in Figure 3 exhibits a very thin response trajectory shape representing the large amplitude in across-wind vibration at the reduced velocity of 12.5 whereas the CFD result has a similar tendency but smaller absolute response values. The CFD result of the case at (2, 2) also exhibits an elliptic-like shape with smaller amplitudes as the experimental results in Figure 4 under the reduced velocity of 10.8. For the case at (-2, 2) under the reduced velocity of 6.2, a left-elliptic shape is also found in CFD result to be similar to the response trajectory in Figure 5.

By using the same setting of CFD technology, the explanation of the downstream interference effect from (x/D, y/D) = (-2, 0) can

be intuitively attempted. Figure 6 shows that the time history of across-wind displacement has stable cycle.

Figure 7 represents a half cycle series of vorticity patterns from the simulation result of the case at (-2, 0). It is indicated that the downstream interfering model does not become an obstacle to the formation of vortex shedding from the principal building model; instead, the vortex separated from the principal building model converges to the vortex generated from the downstream interfering building model. The channel between the two models is almost constant and it sometimes provides enough space for the clockwise vortex to roll up to the upper surface of the interfering building model or for the counter-clockwise vortex to roll down to the bottom surface of the interfering building model.

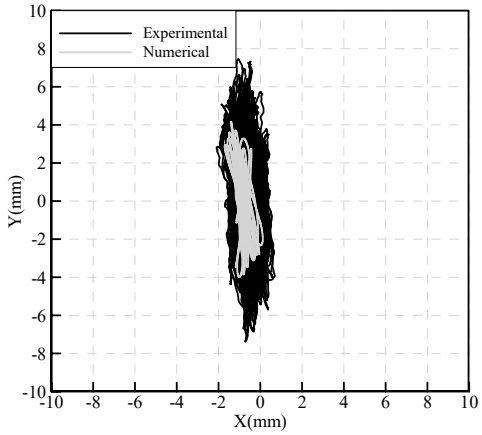

Figure 3. Response trajectory of the case (x/D, y/D) = (-2, 0) under Ur=12.5.

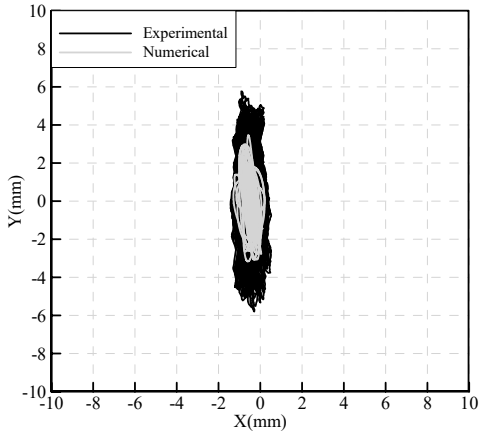

Figure 4. Response trajectory of the case (x/D, y/D) = (2, 2) under Ur=10.8.

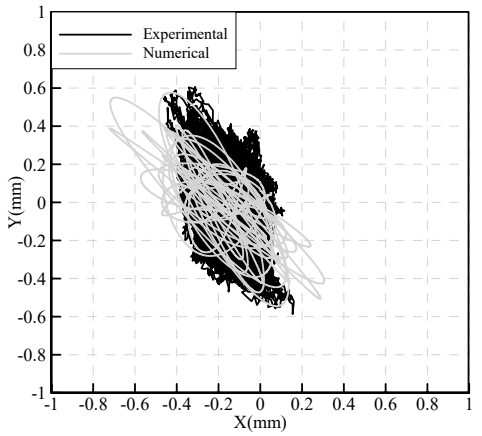

Figure 5. Response trajectory of the case (x/D, y/D) = (-2, 2) under Ur=6.2.

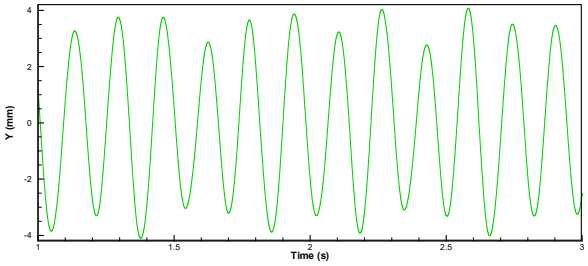

Figure 6. Y displacement time history of the aero-elastic case of (-2, 0) under Ur = 15.9

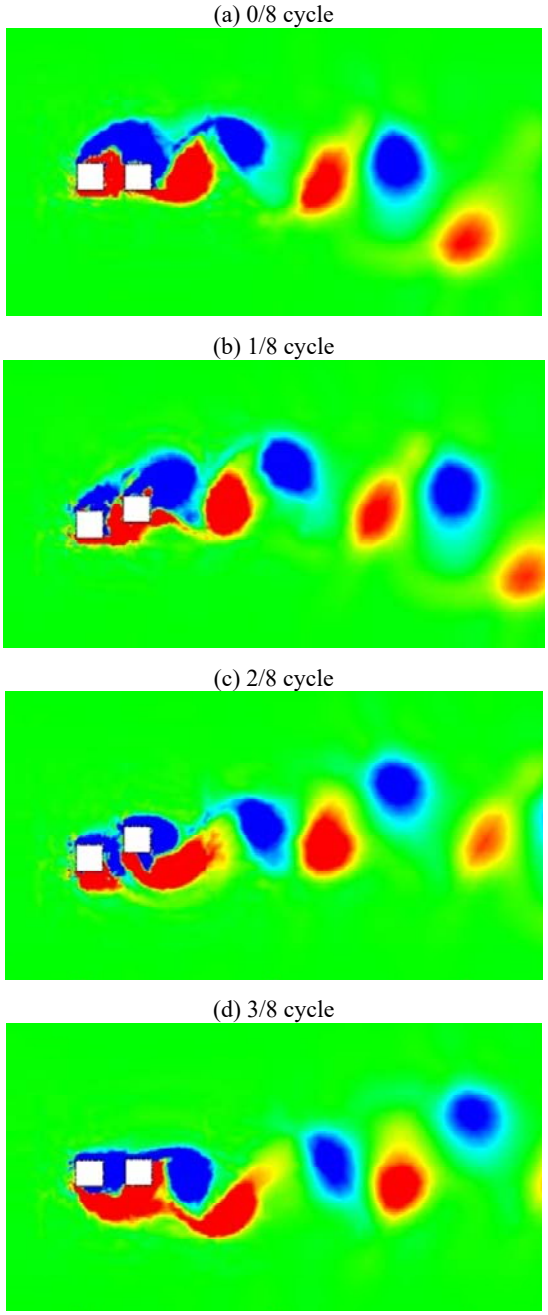

Figure 7. Truncated patterns of vorticities at the aero-elastic case of (-2, 0) under Ur = 15.9 (Blue: counter-clockwise vorticity; Red: clockwise vorticity)

Conclusions

In this study, an idealized 2D FSI simulation with LES model is attempted to simulate the 3D prism interference effect through the motion transform method. 3 typical arrangements simulation are employed to compare the aero-elastic model response trajectory. Although the absolute values from CFD results cannot be perfectly compared with the experimental results, the movement mechanism of the aero-elastic model has good agreement with the experiments. This provides an intuitive way for the observation of the interference mechanism.

References

[1] Asyikin, M.T., *CFD Simulation of Vortex Induced Vibration of a Cylindrical Structure*, Department of Civil and Transport Engineering, Norwegian University of Science and Technology, 2012.

[2] Bouris, D. & Bergeles, G., 2D LES of vortex shedding from a square cylinder, *J. Wind Eng. Ind. Aerodyn.*,**80**, 1999, 31–46.

[3] Lo, Y.L., Kim, Y.C. & Li, Y.C., Downstream Interference Effect of High-rise Buildings under Turbulent Boundary Layer Flow, *J. Wind Eng. Ind. Aerodyn.*,**159**, 2016, 19-35.

[4] Lilly, D.K., A proposed modification of the Germano subgrid-scale closure model, *Phys. Fluids*,**4**, 1992, 633–635.

[5] Noda, H. & Nakayama, A., Reproducibility of flow past two-dimensional rectangular cylinders in a homogeneous turbulent flow by LES, *J. Wind Eng. Ind. Aerodyn.*,**91**, 2003, 265–278.

[6] Vikram, C.K., Krishne Gowda, Y.T., Ravindra, H.V. & Gangadara Gowda, C.J., Manu, Numerical simulation of two dimensional unsteady flow past two square cylinders, *Int. J. Technol. Eng. Syst*.,**2(3)**, 2011, 355–360.